

Top seeded melt growth of Gd–Ba–Cu–O single grain superconductors

This article has been downloaded from IOPscience. Please scroll down to see the full text article.

2010 Supercond. Sci. Technol. 23 034008

(<http://iopscience.iop.org/0953-2048/23/3/034008>)

View [the table of contents for this issue](#), or go to the [journal homepage](#) for more

Download details:

IP Address: 207.255.40.131

The article was downloaded on 24/11/2010 at 19:45

Please note that [terms and conditions apply](#).

Top seeded melt growth of Gd–Ba–Cu–O single grain superconductors

D A Cardwell¹, Y-H Shi¹, N Hari Babu², S K Pathak¹, A R Dennis¹
and K Iida³

¹ Superconductivity Group, Engineering Department, University of Cambridge,
Cambridge CB2 1PZ, UK

² Brunel Centre for Advanced Solidification Technology (BCAST), Brunel University,
West London UB8 3PH, UK

³ The Leibniz Institute for Solid State and Materials Research Dresden (IFW)-Dresden,
01069 Dresden, Germany

Received 8 September 2009, in final form 5 October 2009

Published 22 February 2010

Online at stacks.iop.org/SUST/23/034008

Abstract

Top seeded melt growth (TSMG) has been used extensively to fabricate large, single grain Y–Ba–Cu–O (YBCO) bulk superconductors that can trap large magnetic fields. The TSMG method is relatively economical and has enabled the development of batch processes for the fabrication of a large number of bulk single grain superconductors in a single furnace. In addition, the technique allows the fabrication of complex-shaped bulk samples with controlled and strongly connected grains by using a novel, multi-seeding process. A practical processing route for processing of LRE–Ba–Cu–O (where LRE represents a light rare earth element) single grain superconductors (which have superior properties to YBCO) has been developed at Cambridge over the past three years, based on the development of a generic seed of melt textured Mg-doped Nd-123 and suppression of solid solution phase formation in air by enriching the precursor composition with excess Ba. In this paper we report the successful application of a practical TSMG process in the fabrication of high performance Gd–Ba–Cu–O (GdBCO) single grain superconductor. This method has enabled the development of a batch process for GdBCO and we demonstrate for the first time the fabrication of a large number of high performance single grains of this material in a single process. Finally, we report the processing of bulk GdBCO in the form of complex geometries with controlled grain orientation for bespoke engineering applications.

(Some figures in this article are in colour only in the electronic version)

1. Introduction

The top seeded melt growth (TSMG) process [1] has been used extensively to fabricate large, single grain Y–Ba–Cu–O (YBCO) superconductors that can trap large magnetic fields of up to 17 T at 29 K in a two sample arrangement [2–4]. The TSMG process involves placing a seed crystal, such as Nd–Ba–Cu–O (NdBCO) or Sm–Ba–Cu–O (SmBCO), on the top surface of a YBCO precursor pellet, partially melting the arrangement in an air atmosphere and, finally, peritectic solidification of the melt at around 1015 °C. This melt-processing technique is relatively economical and has enabled the development of a batch process for the fabrication of a large number of YBCO bulk single grain superconductors in a single furnace [5, 6]. In addition, the TSMG process enables the

fabrication of bulk samples of complex shapes with strongly connected grains of controlled orientation by a multi-seeding process. The potential of large YBCO grains fabricated by this process for a variety of engineering applications has been established [7–9].

In general, the performance of (LRE)–Ba–Cu–O ((LRE)BCO, where LRE is a light rare earth element) superconductors is superior to that of YBCO. A practical processing route for the fabrication of (LRE)BCO single grain, bulk superconductors has been developed at the Department of Engineering, University of Cambridge over the past 4 years [10], based on the discovery of a generic seed of Mg-doped NdBCO [11] and suppressing the formation of a Ba/LRE solid solution phase in air by enriching the precursor

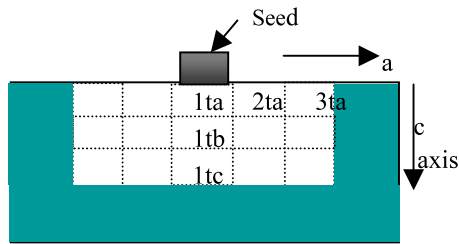


Figure 1. Schematic illustration of the cross-section of a single grain and the position of sub-specimens along the a and c -axes of a single GdBCO grain cut for magnetic T_c and J_c measurements using a SQUID magnetometer.

powder with Ba [10, 12]. This process is directly analogous to the TSMG process used to process YBCO. In this paper, we describe the development of the modified TSMG process for fabrication of high performance GdBCO single grain bulk superconductors, both in the form of individual samples and as part of a batch process. We demonstrate for the first time that a large number of high performance, Gd–Ba–Cu–O single grains can be fabricated simultaneously by a similar batch process to that developed for YBCO. In addition, we demonstrate further that bulk GdBCO can be fabricated in the form of relatively complex shapes with grains of controlled orientation.

2. Experimental details

The generic seed crystals used in this study were fabricated by a conventional melt process technique [13]. Initially, precursor powder with a starting composition of $\text{NdBa}_2\text{Cu}_3\text{O}_7$ (Nd-123) + 12 mol% $\text{Nd}_4\text{Ba}_2\text{Cu}_2\text{O}_{10}$ (Nd-422) + 1 wt% MgO was pressed uniaxially into a pellet and melt processed without the use of a seed crystal under air. The resultant melt-processed pellet typically contained randomly oriented, multi-grains that could be cleaved easily along their crystallographic ab -planes to produce a large number of small, single grains [13]. These were used to process the following compositions of GdBCO by the TSMG technique:

- (i) 70 wt% Gd-123 + 30 wt% Gd-211 + 0.1 wt% Pt + X wt% BaO_2 ; $X = 0, 1, 2$ and 4;
- (ii) $(100-Y)$ wt% Gd-123 + Y wt% Gd-211 + 0.1 wt% Pt + 1 wt% BaO_2 ; $Y = 20, 25$ and 30;
- (iii) $(75 \text{ wt% Gd-123} + 25 \text{ wt% Gd-211} + 0.1 \text{ wt% Pt}) + 10 \text{ wt% Ag}_2\text{O} + 1 \text{ wt% BaO}_2$.

Green pressed pellets of diameters between 20 and 30 mm of the above compositions were placed onto ZrO_2 supporting rods inside a conventional box furnace. A generic seed of 1 wt% MgO–NdBCO was placed on the top of the pellet to nucleate the growth of a single grain. The arrangement was heated to 1070 °C, maintained at this temperature for 1.0 h and then cooled rapidly to 1036 °C, at about 140 °C h⁻¹. Finally, the pellets were cooled slowly at a rate of 0.3 °C h⁻¹ to 998 °C and then cooled further at 300 °C h⁻¹ to room temperature. The same thermal profile was used for batch processing and for the multi-seeding process.

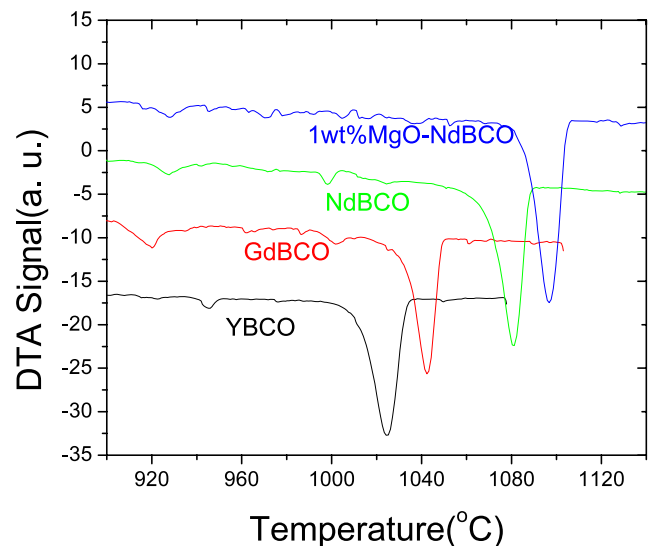


Figure 2. Differential thermal analysis of a Nd–Ba–Cu–O melt textured sample containing 1 wt% MgO. DTA traces of Nd-123, Sm-123 and Gd-123 are also shown for comparison.

Bulk GdBCO cavities were fabricated by TSMG in two different ways using precursor composition (iii). In the first method, a blind hole was drilled into a cylindrical pellet, formed by pressing uniaxially and sintering the precursor powder at 910 °C for 6 h, using a lathe. In the second method, the powder was pressed into the required geometry using a ram and die assembly. A thin, uniaxially pressed disc of the same composition was placed on the open end of the cavity prior to melt processing to yield a closed cavity in the fully processed sample. A generic Mg-doped NdBCO seed crystal was used to seed the growth of the cavity in a way similar to the fabrication of single grains (i.e. using a similar temperature profile). Finally, the individual melt-processed single grains, batch-processed single grains, multi-seeded grains and seeded, melt-processed cavities were oxygenated in a tube furnace at temperature between 360 and 440 °C for 150 h.

Smaller single grains (16 mm in diameter after melt processing) were cut into two halves perpendicular to their a – b plane (i.e. through the thickness of the single grain). One half of the grain was polished to expose its microstructure and the other was cut into small pieces ($1.0 \times 1.0 \times 0.5 \text{ mm}^3$) for measurement of the superconducting properties of the sample, such as transition temperature, T_c , and critical current density, J_c . The individual specimens cut from the top region of the a -growth sector are labelled schematically in figure 1 as 1ta, 2ta, 3ta etc, and those from the c -growth sector as 1ta, 1tb, 1tc, etc. A MPMS XL SQUID magnetometer was used to measure the magnetic moment as a function of temperature and the magnetic hysteresis loops of these specimens, with the extended Bean model used to calculate J_c from the latter. Larger single grains (26 mm diameter after melt processing) were used for trapped field measurements. This involved cooling the samples initially to 77 K using liquid nitrogen, followed by magnetization in an applied field of 3 T. A Hall probe positioned 0.2 mm above the sample surface was

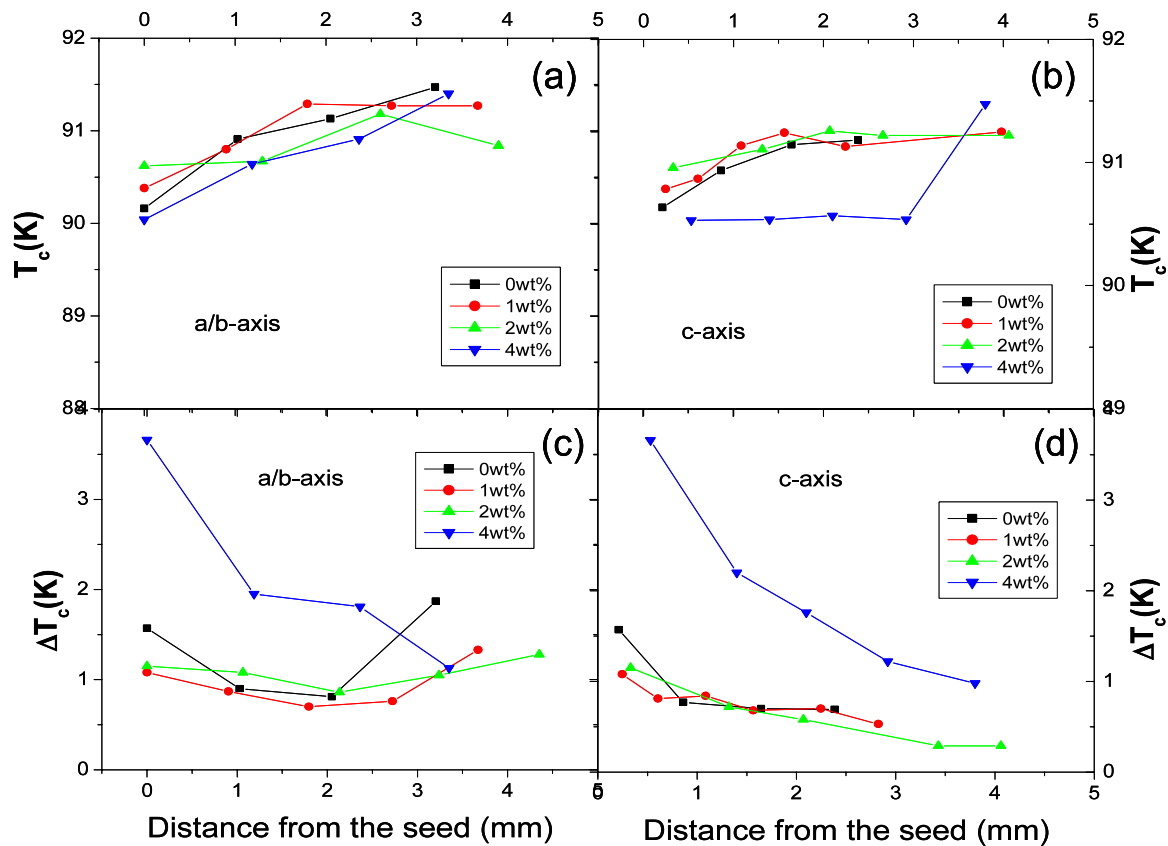


Figure 3. Spatial variation of T_c and ΔT_c for GdBCO single grains fabricated from starting compositions of 70 wt% Gd-123 + 30 wt% Gd-211 + X wt% BaO₂ + 0.1 wt% Pt, where $X = 0, 1, 2, 4$. (a) and (b) show the variation in T_c along the a and c -axes; (c) and (d) show the variation in ΔT_c along the a and c -axes.

scanned over the entire single grain after the applied field was removed. The trapped magnetic field of the multi-seeded grain was measured in a field-cooled (FC) process, which involved cooling the sample in an applied field of 0.5 T using a permanent magnet of diameter 32 mm and, again, measuring the trapped magnetic field with Hall probe following removal of the external field.

3. Results and discussion

The differential thermal analysis (DTA) trace for the Mg-doped NdBCO generic seed crystal is compared with Nd-123, Gd-123 and Y-123 in figure 2. The melting point of the generic seed is 15 °C higher than that of Nd-123, which has the highest melting temperature of the various (RE)BCO systems, suggesting that this seed can be used potentially to grow of any (RE)BCO single grain. In addition to exhibiting a significantly higher melting point, the Mg-doped Nd-123 seed crystal has a lattice mismatch of <0.7% in the a/b -direction of the Nd-123 crystallographic lattice [13]. Such a small mismatch between Mg-doped Nd-123 and the target RE-123 phase can result potentially in the epitaxial growth of any RE-123 phase compound if the former is used as a seed crystal.

The variation of transition temperature within GdBCO single grains fabricated from composition (i) precursor was measured using the MPMS XL SQUID magnetometer. It can

be seen from figures 3(a) and (b) that T_c within a seeded grain melt processed from a precursor pellet without excess BaO₂ increases from 90.5 to 91.5 K with increasing distance from the seed crystal along the a - or c -axes. The spatial variation of transition width, ΔT_c , along the a and c -axes is shown in figures 3(c) and (d). Relatively broad transitions are observed in the vicinity of the seed (i.e. under the initial grain formation conditions at the position of the seed). The observation of a lower T_c and broader transition width in the vicinity of the seed, both along the a and c -axes of the sample (figures 3(c) and (d)), compared to that observed in the region more distant from the seed, suggests that the Gd/Ba solid solution phase forms during only the initial stage of crystal growth. It is known that the maximum value of x in the $\text{Gd}_{1+x}\text{Ba}_{2-x}\text{Cu}_3\text{O}_{7-\delta}$ solid solution phase can be as high as 0.1 [14], with x decreasing as the growth of Gd-123 phase proceeds [15]. The addition of 1 wt% or 2 wt% BaO₂ to the precursor powder effectively increases the local T_c at the position of the seed and reduces ΔT_c compared with the sample fabricated without additional BaO₂. This result suggests that the addition of BaO₂ suppresses the formation of the solid solution phase. The T_c s for the specimens cut from the sample containing 1 wt% BaO₂ are observed to be 92 K along the a -axis of the entire single grain, providing further evidence that the addition of a small amount of BaO₂ to the precursor powder is effective in suppressing Gd/Ba substitution, i.e. the value of x in the formula $\text{Gd}_{1+x}\text{Ba}_{2-x}\text{Cu}_3\text{O}_{7-\delta}$ decreases for an added

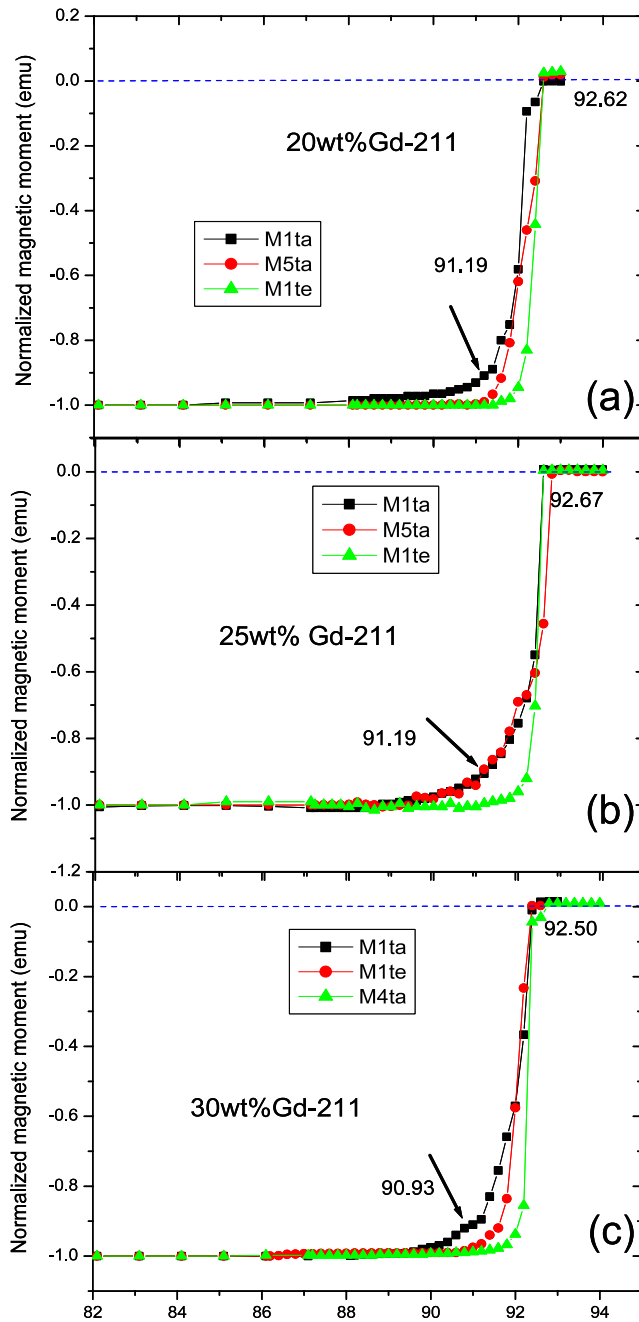


Figure 4. Distribution of T_c within the sample for single grains containing different amounts of Gd-211: (a) 20 wt% Gd-211; (b) 25 wt% Gd-211; (c) 30 wt% Gd-211.

BaO₂ content of 1–2 wt%. Although the sub-specimens exhibit good T_c s (~ 91 K, with a typical transition width of ~ 1 K) it has not been possible to grow large single grains of diameter greater than 8–10 mm when the BaO₂ level increases above 2 wt% due to the associated reduction in grain growth rate [16]. The measured values of ΔT_c , however, are observed to increase significantly (figure 3(d)) in the vicinity of the seed crystal. From a processing point of view, therefore, 1 or 2 wt% excess BaO₂ has been identified as the optimum composition range for the fabrication of large single grains that exhibit homogeneous superconducting properties and suppressed levels of Gd/Ba

solid solution formation. Given that the growth rate at a specific level of undercooling decreases as the concentration of BaO₂ increases, however, addition of 1 wt% BaO₂ to the precursor is believed to be optimum for the fabrication of large single GdBCO grains with suppressed solid solution formation.

In order to verify whether the addition of 1 wt% BaO₂ to the GdBCO precursor prior to melt processing is sufficient to suppress significantly Gd/Ba substitution independently of Gd-211 content, several single grains containing various amounts of Gd-211 were fabricated and the distribution of T_c measured at various points in the sample (figures 4(a)–(c)). It can be seen from figure 4(a) that the on-set T_c is uniform across the entire single grain processed from the precursor containing 20 wt% Gd-211. The on-set T_c for this sample is constant for all specimens in the *a*- (samples 1ta and 5ta) and *c*-directions (samples 1ta and 1te). The maximum ΔT_c is 1.41 K at the position under the seed (sample 1ta). Similarly, it can be seen from (b) and (c) that the distribution of T_c is also uniform, with ΔT_c of 1.48 and 1.57 K across single grains containing 25 wt% Gd-211 and 30 wt% Gd-211, respectively. These results indicate that Gd/Ba solid solution, which degrades the superconducting properties of the grains as discussed above, is unaffected by varying the Gd-211 concentration in the precursor composition enriched with 1 wt% BaO₂.

Figures 5(a)–(d) show the distribution of J_c for the single grains containing 20 wt% Gd-211 and 30 wt% Gd-211 along the *a* and *c*-axes. It can be seen that J_c under the seed crystal (1ta) for both samples is the lowest and increases with increasing distance from the seed, both in the *a*- and *c*-directions. J_c values in the *c*-direction are lower than those in the *a*-direction at equivalent positions in the two samples and are generally higher for the sample containing 30 wt% Gd-211, although the range of increase is not large. The observed distribution of J_c inside the single grain is consistent with microstructural studies on YBCO single grains, where the microstructure of a single domain material is inhomogeneous and the concentration of Y-211 particles (i.e. flux pinning centres) in the *c*-growth sector is lower than that in the *a*-growth sector [17]. Furthermore, the results of the present study indicate that the distribution of J_c correlates well with the observed distribution of Gd-211 in the microstructure of the single grains; J_c at low field (< 1 T) increases as the Gd-211 concentration increases from the seed to more distant positions. It can be seen further that the peak effect at higher applied fields (1–2 T) in the *c*-direction is more apparent than that in the *a*-direction for both GdBCO samples due to the reduced concentration of Gd-211 in the *c*-direction. Similarly, the peak effect in the sample containing 20 wt% Gd-211 is more pronounced than that in the sample containing 30 wt% Gd-211. Therefore, a lower Gd-211 concentration is preferred for achieving higher trapped field since J_c at higher field (about 1 T is expected in trapped field measurements for single grains of diameter 26 mm) is particularly important for practical applications. Single grains containing 20 wt% Gd-211 generate more liquid phase during melt-processing making it generally more difficult to maintain the shape of the single grain in these samples. The composition of Gd-211 in the precursor powder for fabricating large single grains that exhibit high trapped field has, therefore, been optimized to be 25 wt%.

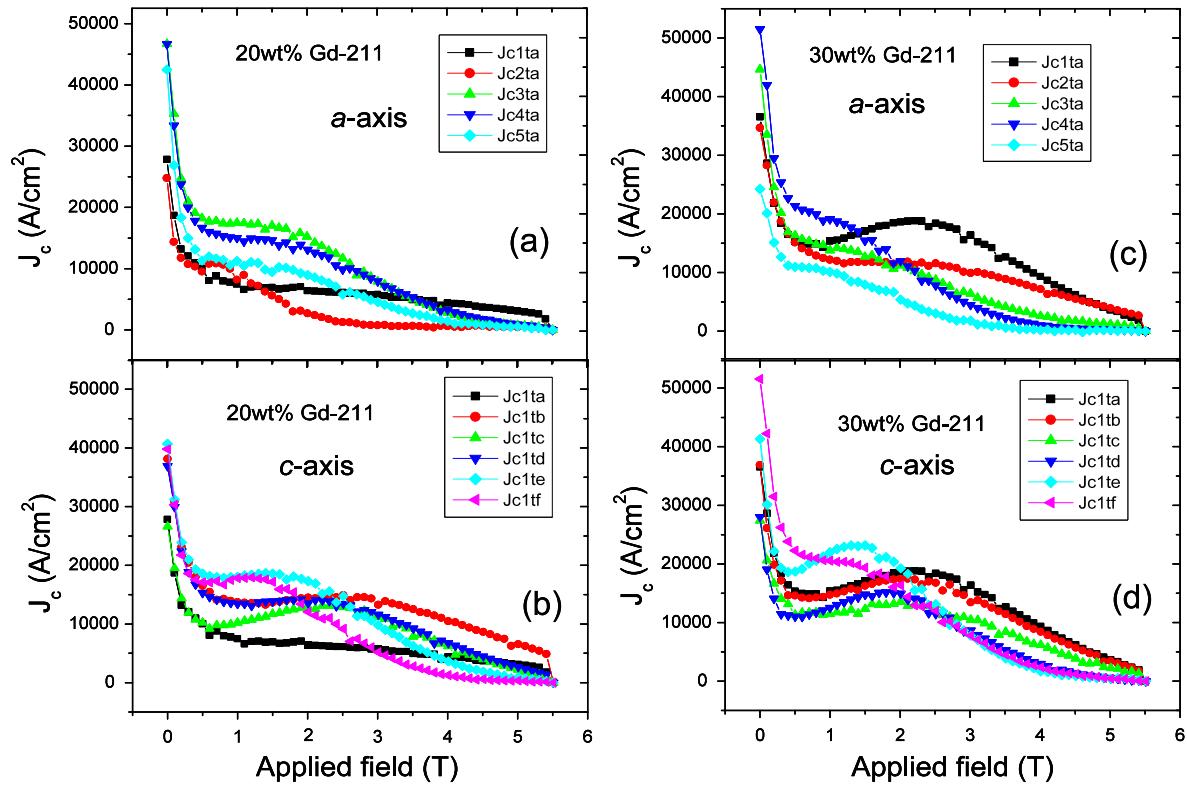


Figure 5. Distribution of J_c along the a - and c -axes of single grains containing 20 wt% Gd-211 and 30 wt% Gd-211, respectively. (a) 20 wt% Gd-211, a -axis. (b) 20 wt% Gd-211, c -axis. (c) 30 wt% Gd-211, a -axis. (d) 30 wt% Gd-211, c -axis.

It is necessary to improve the mechanical properties of the single grain so that magnetized samples can sustain the considerable magnetic pressure and thermal shock experienced during cooling in practical applications. This was achieved by introducing metallic Ag into the single grain microstructure by adding Ag_2O to precursor composition (ii) for $Y = 25$ (to form composition (iii)), as shown in figure 6(b). The introduction of Ag does not change significantly the size and distribution of the Gd-211 phase inclusions in the bulk microstructure, which is shown in figure 6(a). The spatial variation of T_c within the sample was measured to investigate the influence of Ag on the formation of Gd/Ba solid solution. Figure 7 shows the distribution of T_c both in the a - and c -directions. It can be seen that the values of T_c vary within 0.5 K for the whole single grain; ΔT_c varies within 1.5 K in the a -direction and within 1.0 K in the c -direction, with the exception that ΔT_c under the seed is as high as 4 K. This indicates that the solid solution still forms in the region under the seed in the single grain containing Ag, even after the addition of 1.0 wt% BaO_2 to the precursor powder. However, the extent of the region under the seed that exhibits such a broadening of T_c is only about 1.5 mm. This local reduction in T_c will have no significant effect on the field trapping ability of the single grain since super-current loops of relatively small radii make a relatively small contribution to the overall magnetic moment of the bulk sample (magnetic moment scales with the square of the sample radius).

Figure 8 shows that the position-dependent J_c for the sample containing Ag is similar to that of the Ag-free single grain superconductor, i.e. J_c is lowest under the seed, increases

with distance from the seed along both the a - or c -directions and reaches its highest value at the positions close to the edge of the sample. The peak effect is predominant throughout the Ag-containing sample, suggesting that higher trapped magnetic fields can be achieved in a single grain of this composition.

The trapped magnetic field profile of the large single grain (of diameter 26 mm) fabricated by TSMG from a precursor composition of 75 wt% Gd-123 + 25 wt% Gd-211 + 0.1 wt% Pt + 10 wt% Ag_2O + 1 wt% BaO_2 , was measured at 77 K by a field-cooled process with an applied field of 3 T, as shown in figure 9. This single grain exhibits a trapped field of 0.91 T at 77 K, which is the highest value reported to date for a GdBCO single grain of this size melt processed in air, and is comparable with reported values of trapped field of GdBCO single grains processed in reduced O_2 in N_2 (i.e. a conventional process for avoiding the formation of a solid solution). Although, the trapped magnetic fields for large single grains of composition (ii) for $Y = 20$ and 30 have not been measured, the spatial variation of $J_c(B)$ within the samples indicate that the optimum composition for obtaining higher trapped fields in large grain GdBCO is composition (iii). A Gd-211 content of 25 wt% yields higher J_c s in medium applied fields (i.e. the 1–2 T range), and 10 wt% Ag_2O improves the fracture toughness of the sample.

3 kg of powder of composition (iii) was mixed thoroughly using a motorized powder mixer and pressed uniaxially into pellets of various diameters (20, 26 and 32 mm) for batch-processing trials. An Mg-doped NdBCO seed crystal was

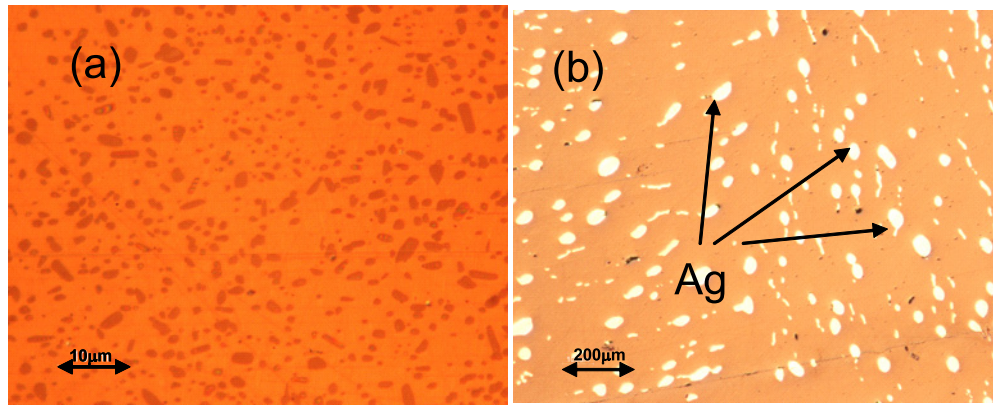


Figure 6. Microstructures of a single grain fabricated from a precursor composition of 75 wt% Gd-123 + 25 wt% Gd-211 + 10 wt% Ag₂O + 1.0 wt% BaO₂ + 0.1 wt% Pt at (a) higher magnification to reveal the size of the Gd-211 inclusions and (b) lower magnification to reveal the distribution of metallic Ag.

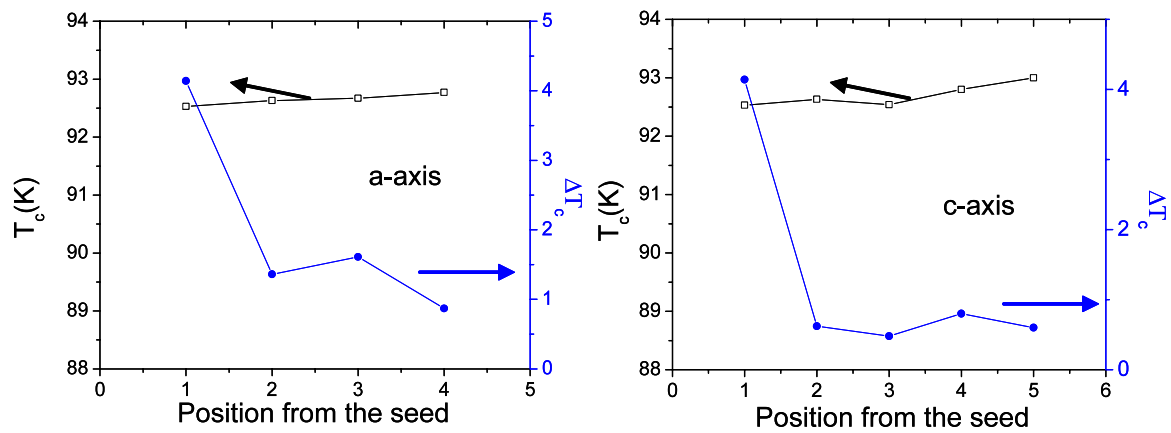


Figure 7. Distribution of T_c and ΔT_c along the a and c -axes of a single grain sample fabricated from a precursor composition of 75 wt% Gd-123 + 25 wt% Gd-211 + 1.0 wt% BaO₂ + 10 wt% Ag₂O + 0.1 wt% Pt.

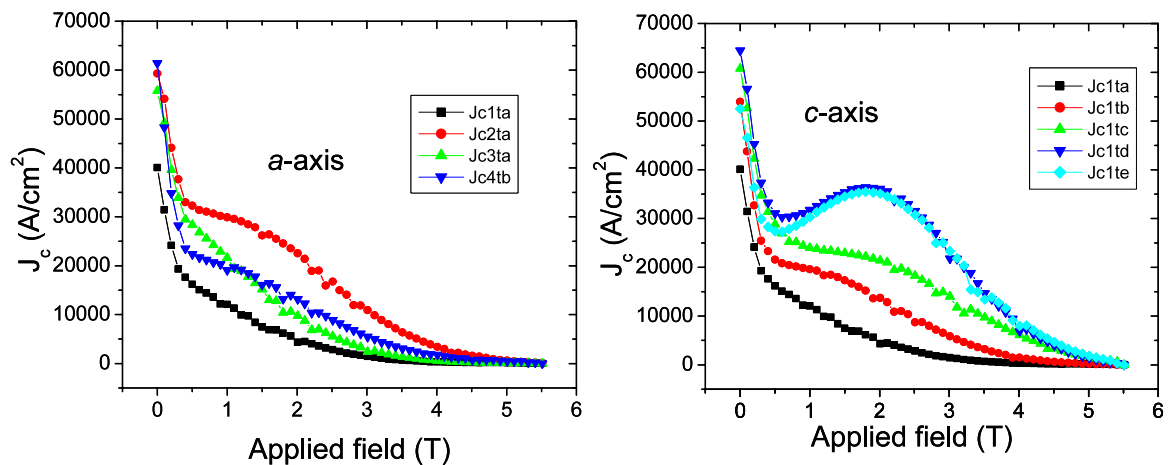


Figure 8. Distribution of J_c along the a and c -axis of a single grain sample fabricated from a precursor composition of 75 wt% Gd-123 + 25 wt% Gd-211 + 1.0 wt% BaO₂ + 10 wt% Ag₂O + 0.1 wt% Pt.

placed on top of the each pellet prior to melt processing. The pellets were then placed on a ceramic plate in a purpose-designed box furnace to batch process YBCO single grain superconductors. The hot zone in this furnace is (H) 20 cm \times (D) 60 cm \times (W) 60 cm, corresponding to a region of uniform

temperature of (H) 10 cm \times (D) 40 cm \times (W) 40 cm (i.e. the active growth zone). Large area heating coils are located on the four vertical sides of the sample chamber and the temperature is sampled at various positions to ensure that a homogeneous lateral thermal distribution within the hot zone

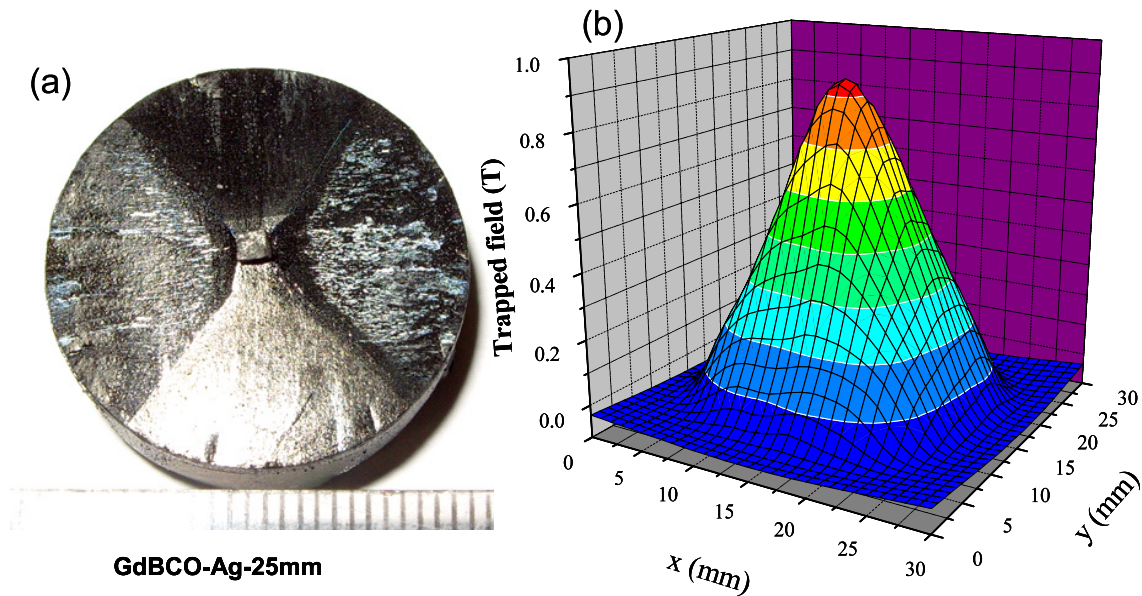


Figure 9. (a) Photograph of a Gd–Ba–Cu–O large single grain (26 mm in diameter) of starting composition 75 wt% Gd-123 + 25 wt% Gd-211 + 1 wt% BaO₂ + 10 wt% Ag₂O + 0.1 wt% Pt fabricated in air. (b) The trapped magnetic field at a distance of 0.2 mm above the surface of this sample. The maximum trapped field is observed to be 0.91 T at 77 K.

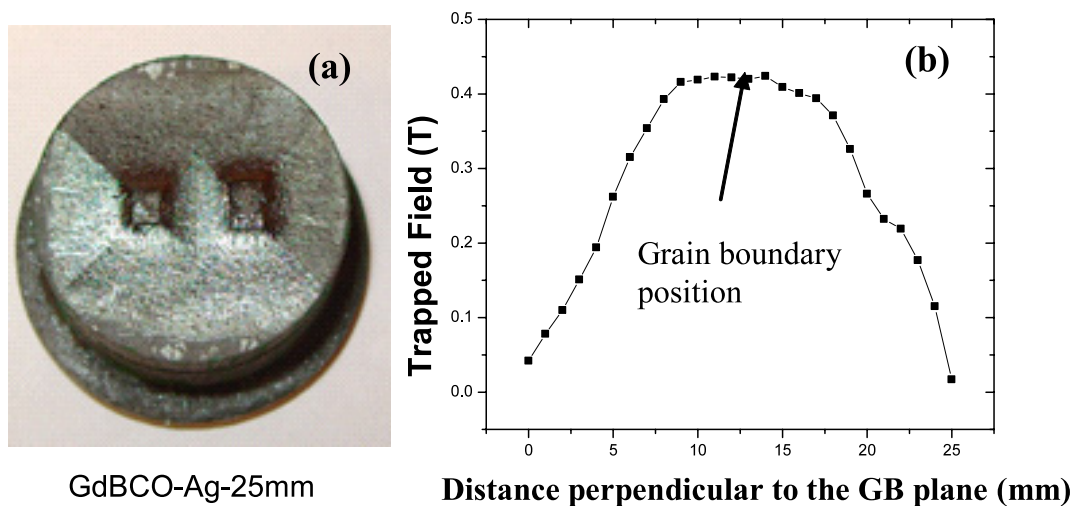


Figure 10. (a) Top view of an oriented grain produced with a multiple (bridge) seed. The photograph was taken after removing seeds from the as-grown sample to reveal the growth facet lines. (b) The trapped magnetic field along the *a/b*-axis measured perpendicular to the grain boundary. A single, inverted parabola with a maximum field position coinciding with that of the GB can be seen, indicating the presence of a strongly coupled GB.

is maintained. The success rate of the Mg-doped seed crystal to act as an effective nucleation point in the GdBCO batch process is very high (effectively 100%). However, the success rate for the complete growth of single grains, without the formation of unwanted satellite nuclei, is highly dependent on internal temperature variations within the furnace. Several batch-processing runs in this furnace for GdBCO samples of composition (iii) have been performed. All the precursor pellets can be grown successfully into single grains during the batch process for an optimized melt-processing temperature profile. Trapped fields are measured for six single grains of 26 mm in diameter and their average trapped field is 0.89 T (± 0.2 T) at 77 K.

The TSMG process for the fabrication of GdBCO single grain superconductors, developed in this study, was used to fabricate GdBCO multi-grains containing artificial grain boundaries. A bridge-shaped seed crystal [18] was cut from a large, single Mg-doped NdBCO grain in order to achieve good alignment between the impinging, separately seeded grains at the grain boundary. This seed crystal simulates a multi-seeding process in which the orientation between two adjacent grains can be controlled precisely. Figure 10(a) shows a photograph of the sample fabricated by the TSMG technique using the bridge-shaped seed crystal. The artificial grain boundary (GB) forms as a result of impinging *ac*-planes of individual grains that nucleate at the different seed contact points. The top



Figure 11. Photograph of a GdBCO cavity fabricated by combining a multi-seeding process and TSMG.

surface of seeded grain following removal of seed can be seen in this figure. Figure 10(b) shows the trapped field measured across the grain boundary. The position of the seed crystal and the GB are marked in the figure. The single, inverted parabolic flux profile apparent in figure 10(b), suggests that the GB supports large currents. The observed maximum value of trapped field (~ 0.3 T) is relatively small compared to that of single GdBCO grains of similar dimensions. It is important to note, however, that this reduced value of trapped field is as a result of an incomplete critical state (i.e. due to the lower applied magnetic field of ~ 0.5 T), rather than to the weak-link nature of grain boundary. The coincidence of the position of the peak with the position of the grain boundary suggests that a single, large current loop circulates around the sample after the magnetization process. Further tests under high field magnetization are in progress to characterize the nature of grain boundary under external magnetic field.

We have attempted to fabricate bulk GdBCO superconductors in complex geometries in order to explore further the TSMG process for the GdBCO system. For this purpose, cavity shaped precursor pellets have been fabricated and Mg-doped NdBCO seed crystals placed at appropriate positions on the upper surface of the cavity bottom and on the top surface of the cavity cover to facilitate heterogeneous nuclei. The precursor pellet and arrangement of seeds was placed in a furnace for melt processing in an air atmosphere. Figure 11 shows a photograph of both ends of the closed cavity; the seeded grain can be seen clearly on top surface of the cavity. The microstructural and superconducting properties of various cavities and complex-shaped GdBCO manufactured using TSMG process will be reported elsewhere. This study demonstrates for the first time, however, that this material can be melt processed effectively into bespoke components for applications such as microwave resonant filters, components for motors and generators and cavity thrust bearings.

4. Conclusion

A top seeded melt growth method has been developed for the fabrication of large grain, bulk Gd–Ba–Cu–O superconductors based on the development of a new type of generic seed crystal (Mg-doped Nd–Ba–Cu–O) that can promote effectively the epitaxial nucleation of any (RE)–Ba–Cu–O system and

by suppressing formation of (Gd)/Ba solid solution in a controlled manner within large Gd–Ba–Cu–O grains processed in air. A systematic investigation of the effect of adding various amounts of BaO₂ on the superconducting properties of large grain samples reveals that the addition of 1 or 2 wt% BaO₂ to the precursor corresponds to an optimum concentration required to achieve high performance single grains melt processed in air. 1 wt% BaO₂ is found to suppress the formation of Gd/Ba solid solution, even under conditions of significant variations of Gd-211 content. Gd–Ba–Cu–O single grain, bulk superconductors processed using the practical processing method described in this study exhibit significantly improved trapped fields. The new process enables the fabrication in air of large grain, bulk superconductors, and particularly LRE–Ba–Cu–O materials that exhibit good superconducting properties. The cold seeding TSMG method has enabled a batch process for Gd–Ba–Cu–O single grains to be developed for the first time, analogous to the batch process developed previously for the Y–Ba–Cu–O system. A multi-seeding technique based on the TSMG process has been used successfully to fabricate several Gd–Ba–Cu–O grains that contain strongly coupled artificial grain boundaries. Finally, the simplicity of the cold seeding process has been exploited to demonstrate that bulk Gd–Ba–Cu–O superconductors can be processed in the form of complex shapes using the generic seed crystal for potential engineering applications.

References

- [1] Cardwell D A 1998 *Mater. Sci. Eng. B* **53** 1
- [2] Tomita M and Murakami M 2003 *Nature* **421** 517
- [3] Gruss S, Fuchs G, Krabbes G, Verges P, Stöver G, Müller K-H, Fink J and Schultz L 2001 *Appl. Phys. Lett.* **79** 3131
- [4] Walter H, Delamare M P, Bringmann B, Leenders A and Freyhardt H C 2000 *J. Mater. Res.* **15** 1231
- [5] Litzkendorf D, Habisreuther T, Bierlich J, Surzhenko O, Zeisberger M, Kracunovska S and Gawalek W 2005 *Supercond. Sci. Technol.* **18** S206
- [6] Gawalek W, Habisreuther T, Zeisberger M, Litzkendorf D, Surzhenko O, Kracunovska S, Prikhna T A, Oswald B, Kovalev L K and Canders W 2004 *Supercond. Sci. Technol.* **17** 1185
- [7] Hull J R, Hanany S, Matsumura T, Johnson B and Jones T 2005 *Supercond. Sci. Technol.* **18** S1
- [8] Miyagawa Y, Kameno H, Takahata R and Ueyama H 1999 *IEEE Trans. Appl. Supercond.* **9** 996

- [9] Oswald B, Best K-J, Setzer M, Söll M, Gawalek W, Gutt A, Kovalev L, Krabbes G, Fisher L and Freyhardt H C 2005 *Supercond. Sci. Technol.* **18** S24
- [10] Hari Babu N, Shi Y, Iida K and Cardwell D A 2005 *Nat. Mater.* **6** 476
- [11] Shi Y, Hari Babu N and Cardwell D A 2005 *Supercond. Sci. Technol.* **18** L13
- [12] Shi Y, Hari Babu N, Iida K and Cardwell D A 2007 *Supercond. Sci. Technol.* **20** 38
- [13] Shi Y, Hari Babu N, Iida K and Cardwell D A 2006 *J. Mater. Res.* **21** 1355
- [14] Xu C, Hu A, Sakai N, Izumi M and Hirabayashi I 2005 *Physica C* **417** 77
- [15] Kambara M, Miyake K, Murata K, Shiohara Y and Umeda T 1998 *Advances in Superconductivity* vol X ed K Osamura and I Hirabayashi (Berlin: Springer) p 729
- [16] Shi Y H, Hari Babu N, Iida K and Cardwell D A 2007 *IEEE Trans. Appl. Supercond.* **17** 2984
- [17] Diko P, Zmorayova K, Granados X, Sandiumenge F and Obradors X 2003 *Physica C* **384** 125
- [18] Hari Babu N, Withnell T D, Iida K and Cardwell D A 2007 *IEEE Trans. Appl. Supercond.* **17** 2949